Technical Note: The Role of Evolving Surface Tension in the Formation of Cloud Droplets

James F. Davies[1], Andreas Zuend[2], Kevin R. Wilson[3]

5 [1]Department of Chemistry, University of California Riverside, CA USA
[2]Department of Atmospheric and Oceanic Sciences, McGill University, Montreal, Quebec, Canada
[3]Chemical Sciences Division, Lawrence Berkeley National Laboratory, Berkeley, CA USA

Correspondence to: James F. Davies (jfdavies@ucr.edu)

Abstract. The role of surface tension (σ) in cloud droplet activation has long been ambiguous. Recent studies have reported observations attributed to the effects of an evolving surface tension in the activation

10 process. However, adoption of a surface-mediated activation mechanism has been slow and many studies continue to neglect the composition-dependence of aerosol/droplet surface tension, using instead a value equal to the surface tension of pure water (σ_w). In this technical note, we clearly describe the fundamental role of surface tension in the activation of multicomponent aerosol particles into cloud droplets. It is demonstrated that the effects of surface tension in the activation process depend primarily on the evolution

15 of surface tension with droplet size, typically varying in the range $0.5\sigma_w \lesssim \sigma \leq \sigma_w$ due to the partitioning of organic species with a high surface affinity. We go on to report some recent laboratory observations that exhibit behavior that may be associated with surface tension effects, and propose a measurement coordinate that will allow surface tension effects to be better identified using standard atmospheric measurement techniques. However, interpreting observations using theory based on surface film and liquid-liquid phase

20 separation models remains a challenge. Our findings highlight the need for experimental measurements that better reveal the role of composition-dependent surface tensions, critical for advancing predictive theories and parameterizations of cloud droplet activation.

25

Atmospheric
Chemistry
and Physics

Discussions

1 Introduction

The formation of a cloud involves a complex series of steps as nanometer sized aerosol particles, termed

cloud condensation nuclei (CCN), grow by condensation of water vapor to become supermicron-sized cloud

droplets, in a process known as CCN activation. Activation depends on physicochemical properties of the

30   aerosol, such as hygroscopicity and surface tension, as well as atmospheric conditions, such as temperature

and humidity. To accurately predict cloud formation and properties, these factors must be included in

modelling schemes. However, due to computational limitations, approximations and simplifications are

needed, which often obscures the underlying physics and may limit the accuracy of predictions. A key

challenge is in the development of a simple model that captures the basic processes involved in CCN

35   activation, while allowing complicating factors such as surface tension variability, solubility and phase

separation to be included in a physically representative manner. In this note, we focus on the role of surface

tension, and discuss the limitations of current approximations in light of recently published works that

reveal how it is primarily the evolution of surface tension that impacts the activation process.

In recent publications, the role of surface tension in the activation of aerosol particles to cloud droplets has

40   been reexamined (Ovadnevaite et al., 2017; Ruehl et al., 2016). These studies show that the evolution of

surface tension can have a large effect during the activation process compared to when surface tension is

assumed to be a static parameter. It is well established that surface tension is a factor in activation, and that

dissolved species can suppress surface tension (Li et al., 1998). Traditionally, however, surface tension has

been reduced to a fixed term in the Köhler equation (Abdul-Razzak and Ghan, 2000; Facchini et al., 1999;

45   Petters and Kreidenweis, 2007), and is usually given a temperature-independent value equal to that of pure

water at 25 °C. This is because for any decrease in surface tension due to bulk–surface partitioning and

surface adsorption, it is assumed that there is an increase in the solution water activity because adsorbed

material, previously acting as a hygroscopic solute, is removed from the droplet (bulk) solution (Fuentes et

al., 2011; Prisle et al., 2008; Sorjamaa et al., 2004). Thus, the effects approximately cancel out in the

50   calculation of a droplet's equilibrium saturation ratio via the Köhler equation and so are often neglected.

Furthermore, it has been shown in some cases that there is insufficient material in a droplet at the sizes approaching activation to sustain a surface tension depression (Asa-Awuku et al., 2009; Prisle et al., 2010). The lack of experimental evidence to the contrary has led to the adoption of these assumptions in popular single-parameters models, such as κ-Köhler theory, that reduce the complexity of the activation process

55   (Petters and Kreidenweis, 2007). These parameterizations provide a compact and useful means of relating key observables, such as the critical supersaturation and activation diameter, to hygroscopicity and allow a general comparison between systems with arbitrary compositions. The κ-Köhler framework has also been adapted to account for surface tension effects (Petters and Kreidenweis, 2013). However, a single parameter implementation cannot account for the full effects of an evolving surface tension and, by omitting the

60   microphysical processes associated with bulk–surface partitioning, the presence and magnitudes of any surface effects are often difficult to ascertain.

In the works of Ruehl and coworkers (Ruehl et al., 2016; Ruehl and Wilson, 2014), Forestieri and coworkers (Forestieri et al., 2018) and Ovadnevaite and coworkers (Ovadnevaite et al., 2017), laboratory and observation-based measurements, respectively, combined with a partitioning model have revealed key

65   signatures of surface tension lowering in the activation process due to non-surfactant organic compounds. Notably, that a modification of the Köhler curve can result in lower critical supersaturations and vastly different droplet sizes at activation compared to the expectation when assuming a constant surface tension. Dynamic factors may also play a role, as discussed by Nozière and coworkers (Nozière et al., 2014) who have shown that surface tension can vary over time due to slow changes in the bulk-surface partitioning of

70   material, leading to a time-dependence in the role of surface tension. This may be especially important for droplets that initially contain micelles or oligomers that exhibit slow breakdown kinetics and diffusion. Furthermore, surface partitioning may be influenced by non-surface active components in the system, such as the presence of inorganic material (Asa-Awuku et al., 2008; Boyer et al., 2016; Boyer and Dutcher, 2017; Petters and Petters, 2016; Wang et al., 2014). Other factors that have been shown to influence the shape of

75   Köhler curves are: (1) solute dissolution, encompassing both water-solubility and solubility kinetics (Asa-

Awuku and Nenes, 2007; McFiggans et al., 2006; Petters and Kreidenweis, 2013), (2) liquid–liquid phase separation (i.e. limited liquid–liquid solubility) (Rastak et al., 2017; Renbaum-Wolff et al., 2016), and (3) the dynamic condensation (or gas–particle partitioning) of organic vapors (Topping et al., 2013; Topping and McFiggans, 2012). While measured cloud droplet number concentrations in the atmosphere have been

80   explained with simple parameterizations that neglect surface effects (Nguyen et al., 2017; Petters et al., 2016), there are many observations that cannot be explained in such simple terms (Collins et al., 2016; Good et al., 2010; Ovadnevaite et al., 2011; Yakobi-Hancock et al., 2014). In order to gain a robust and predictive understanding of CCN activation, a molecular-level theory must be developed and adopted by the atmospheric chemistry community.

85   In this technical note, we offer a perspective on the role of surface tension in the activation process, drawing on recent studies and interpretations of cloud droplet activation measurements (e.g. (Forestieri et al., 2018; Ovadnevaite et al., 2017; Ruehl et al., 2016; Ruehl and Wilson, 2014)). We go on to discuss how surface tension may be considered in the activation process, and finally present some new data highlighting potential indicators of surface tension effects in measurements of critical supersaturation. Our aim is to

90   provide a platform for discussion and help foster a molecular-based interpretation of the role of organic material in the activation of aerosol to cloud droplets.

2 Clarifying how Surface Tension Alters Cloud Droplet Activation

On a fundamental level, the influence of surface tension on droplet activation is straightforward and was discussed in the late 1990's for aerosol particles containing surfactants (Li et al., 1998). Unfortunately, the

95   simplicity of the role of surface tension in CCN activation has been lost in the complex descriptions of surface and phase-partitioning models, limiting the broader application of the insights gained from recent experimental results. For context, we begin our discussion with Köhler theory (Köhler, 1936), which describes the thermodynamic conditions required for CCN activation based on two contributions that control the equilibrium (saturation) vapor pressure of water above a liquid surface. The classic Köhler

100   equation is often written as (Petters and Kreidenweis, 2007):

$$S_d = \frac{p_{w,d}(\mathrm{D})}{p_w^0} = a_w \exp\left[\frac{4\,M_w\,\sigma}{RT\rho_w \mathrm{D}}\right], \tag{1}$$

where S_d is the equilibrium saturation ratio of water in the vapor phase surrounding a droplet surface, $p_{w,d}$ (D) is the equilibrium partial pressure of water vapor above a droplet (subscript d) of diameter D and a certain chemical composition, p_w^0 is the pressure of water above a flat, macroscopic surface of pure liquid

105 water at temperature T, a_w is the mole-fraction-based water activity of the droplet solution, M_w is the molecular mass of water, σ is the surface tension of the particle (at air-liquid interface), R is the ideal gas constant, and ρ_w is the density of liquid water at T. The water activity contribution, known as the solute or Raoult effect, describes a lowering of the equilibrium water vapor pressure above a liquid surface due to the presence of dissolved (hygroscopic) species that reduce the water activity to a value below 1. The second

110 contribution, known as the Kelvin effect, describes an increase in the equilibrium water vapor pressure above a microscopic curved surface and is dependent upon the surface area-to-volume ratio of the droplet (a size effect) and the surface tension, i.e. the gas-liquid interfacial energy per unit area of surface. The latter term arises from the energy associated with creating and maintaining a certain surface area and, thus, is reduced when the surface tension is lowered or when the droplet size increases, leading to a smaller

115 surface-to-volume ratio. The magnitude of the Kelvin effect scales with the inverse of the droplet radius and is sometimes referred to as the "curvature effect". The combined contributions from the Raoult and Kelvin effects in Köhler theory define a thermodynamic barrier to droplet growth. It is important to note that the Köhler equation describes the specific saturation ratio S_d in thermodynamic equilibrium with a certain solution droplet of interest; however, the value of S_d may differ from that of the environmental

120 saturation ratio, S_{env}, present in the air parcel containing the droplet, since S_{env} is established by an interplay of moist thermodynamic processes. The environmental saturation ratio is defined by $S_{\mathrm{env}} = \frac{p_w}{p_w^0}$, where p_w is the partial pressure of water in air at a specific location and time, irrespective of the presence or absence of aerosols and cloud droplets. The global maximum in a Köhler curve marks the point of activation for a certain CCN, as shown in Figure 1A. For conditions of $S_d \leq S_{\mathrm{env}}$, e.g. in a rising,

125 adiabatically expanding air parcel, aqueous CCN equilibrate relatively quickly to their environmental

conditions such that $S_d = S_{env}$ is maintained (stable growth/evaporation). However, when S_{env} exceeds

the global maximum in S_d for a certain CCN, such an equilibration becomes unattainable and net

condensation of water prevails, leading to so-called unstable condensational growth for as long as $S_{env} >$

S_d holds (while S_d varies according to the pertaining Köhler curve).

130 A Köhler curve shows the relationship between the droplet's equilibrium water vapor saturation ratio and

the wet droplet size. The wet droplet size, or more specifically the chemical composition (solute

concentration), solubility and non-ideal mixing determines the water activity, while the size and surface

tension determine the Kelvin effect. Since the solute concentration changes with the droplet size, e.g. during

net growth conditions when the environmental saturation ratio in an air parcel increases and water vapor

135 condenses, the water activity term varies accordingly, typically in a non-linear manner. The Kelvin term

should also change with droplet size, both due to the changing surface-to-volume ratio of the droplet and

changes in surface tension as a result of changes in solute concentration and related surface composition.

In most scenarios, only the diameter change is accounted for while the surface tension is assumed to remain

constant, usually with the value for pure water ($\sigma = \sigma_w \approx 72$ mN m^{-1} at 298 K). This oversimplifies the

140 problem, especially when organic solutes are present that adsorb at the surface of the growing droplet. In

experimental studies where only the critical supersaturation or critical dry diameter are measured, this

assumption can lead to errors, as the complexity of the system may not allow for such simplified treatments

to yield sufficiently accurate representations of a real-world problem. In such cases, one must consider how

the changing size of the droplet (or, again, more specifically the solution composition) results in changes

145 in bulk-surface partitioning and ultimately surface tension.

Recent work has shown that a rigorous account of bulk–surface partitioning leads to complex Köhler curves

whose shapes are often difficult to interpret (Ruehl et al., 2016). These shapes can be more easily understood

by considering a very simple example, shown in Figure 1B. Here, a series of fixed surface tension (*iso-σ*)

Köhler curves with values ranging from 72 mN m^{-1} to 30 mN m^{-1} are shown, using the same 50 nm particle

Atmospheric
Chemistry
and Physics
Discussions

Open Access

150   (of ammonium sulfate) from Figure 1A. Distinct schematic dependences of the surface tension on the

droplet size are imposed for the purpose of illustration, shown in the lower panel of Figure 1B. At each

point along these dependences, the saturation ratio will be determined by the position on the Köhler curve

corresponding to that specific surface tension. This means that instead of following a single trajectory along

an iso-σ curve, the system is better envisioned as traversing across these curves, producing a very different

155   final shape to the Köhler curve than would normally be expected. In the case of a linear dependence of σ

on D (black curve), the Köhler curve cuts across the iso-σ lines until σ reaches the value of pure water. In

this case, this coincides with reaching the maximum in the droplet's saturation ratio and thus reflects the

activation point. In the case shown in red, activation occurs prior to the surface tension returning to the

value of pure water. In the case shown in green, activation follows a pseudo two-step process, where initially

160   a large increase in size occurs for a small increase in supersaturation, and thus the droplet may appear to be

activated, while in this case true activation occurs at the point corresponding to the intersection with the

Köhler curve of $\sigma = \sigma_w$. It is important to note that it is not necessarily the magnitude of the suppression of

surface tension that drives unusual activation behavior, but the dependence of the surface tension on

concentration, which is dictated by the droplet size and the thermodynamics of the system.

165   It is apparent from these examples that an evolving surface tension may introduce discontinuities in the

activation process that arise due to the phase behavior of monolayer systems. The most obvious

discontinuity is where the surface tension returns to the value of pure water. Following this point, the system

will follow the iso-σ curve corresponding to pure water surface tension (under continued and sufficient

supersaturation conditions). Depending on the exact relationship of surface tension and droplet size, this

170   point can mark the activation barrier of the system, as is the case in Figure 1B for the black and green

curves. This also seemingly supports previous assertions that surface tension does not impact activation,

since it is generally argued that at the point of activation the droplet is sufficiently dilute and essentially

exhibits a surface tension like pure water. While that is the case in this example, the trajectory of the

activation process is significantly altered by the surface tension history of the droplet. In other words, for

175   the systems described by the black or green curves in Fig. 1B, the surface tension at the point of CCN

activation is that of pure water, yet if one would assume the surface tension of the droplet to be constantly

that of pure water at any size prior to activation, the critical supersaturation, SS_{crit}, would be significantly

higher and the critical (wet) activation diameter, D_{crit}, substantially smaller (see the Köhler curve for $\sigma =$

σ_w). Clearly, an evolving surface tension prior to activation can matter in such systems and knowing the

180   surface tension only at the point of activation is insufficient to determine the critical properties at activation,

as well as whether such a droplet of given dry diameter activates for a given environmental peak

supersaturation. The second discontinuity occurs when the surface tension is at its minimum value,

corresponding to a compressed monolayer film at high solute concentration and small droplet size. Again,

in this region the system follows an iso-σ curve before the droplet size grows to the point where the film

185   begins to expand and the surface tension starts increasing, as encountered in typical pressure-area isotherms.

3 Surface Tension Evolution During Activation

A major consequence of an evolving surface tension is that the droplet size at activation is larger, and the

actual critical supersaturation depends on how surface tension varies in the droplet as it grows. These effects

were directly measured using a thermal gradient chamber (TGC) (Roberts and Nenes, 2005; Ruehl et al.,

190   2016). In the 2016 work, mixed ammonium sulfate and organic aerosols were introduced into the TGC at

various supersaturations (up to and including the activation supersaturation). The size of the aerosol

particles was measured under these conditions, allowing a direct measurement of the stable equilibrium

branch of the Köhler curve (i.e. the size up to the point of activation). It was shown that for highly soluble

and surface inactive solutes such as ammonium sulfate and sucrose, the data exhibit the behavior expected

195   when assuming an iso-σ Köhler curve. However, for the case when organic acids, spanning a range of

water-solubilities, were coated on ammonium sulfate particles of specific dry sizes, the measurements

clearly show modifications to the Köhler curve in comparison to an iso-σ Köhler curve, which were

explained by changes in surface tension corresponding to bulk-surface partitioning as predicted by a

compressed film model. Without these observations, assuming $\sigma = \sigma_w$, one could attribute the critical

200 supersaturation to a single, apparent κ value that describes the hygroscopic effect of the mixture of solutes

in the absence of any surface tension constraints (Petters and Kreidenweis, 2007). Low solubility and low

hygroscopicity species should exhibit very small κ values. However, in the case of suberic acid, for

example, the CCN activation data of Ruehl et al. would require a κ value of approximately 0.5 for the

organic component, assuming a fixed surface tension equal to that of water. This κ value is unphysically

205 large considering that the molar volume ratio suggests a value of ~0.13 for suberic acid when assuming full

solubility, the surface tension of pure water and ideal mixing with water. A different prediction, accounting

for limited solubility and assuming a constant surface tension using the value of the saturated aqueous

solution, estimates its value as $\kappa \approx 0.003$ (Kuwata et al., 2013). Moreover, the apparent κ value derived

from CCN activation data of pure suberic acid particles indicates a value of ~0.001 (Kuwata et al., 2013).

210 Invoking a surface tension model here is the only way to make physical sense of these observations,

allowing even low solubility and non-hygroscopic solutes to contribute significantly to the activation

efficiency in mixed droplets. The modelling approaches of Ruehl and coworkers (Ruehl et al., 2016) and

Ovadnevaite and coworkers (Ovadnevaite et al., 2017) use Köhler theory with either a bulk–surface

partitioning model (compressed film model) or an equilibrium gas–particle partitioning and liquid–liquid

215 phase separation (LLPS) model with variable surface tension. Both studies also employed simplified

organic film models, in which the assumption is made that all organic material resides in a water-free

surface film, as options for comparison with the more sophisticated approaches.

A bulk–surface partitioning model is comprised of two components: a two-dimensional equation of state

that relates the surface tension to the surface concentration, and a corresponding isotherm that relates the

220 surface and bulk solution concentrations. In the work of Ruehl et al., the compressed film (Jura and Harkins,

1946) and Szyszkowski-Langmuir equations of states were compared. The latter has been used in several

studies exploring bulk-surface partitioning in organic aerosol (Prisle et al., 2010; Sorjamaa et al., 2004;

Topping et al., 2007). The compressed film model reproduced the experimental observations, capturing the

complex shapes of the measured Köhler curves. The Szyszkowski-Langmuir method was unable to explain

225   several of the observations, attributed partly to the lack of a two-dimensional phase transition between a

film state and a non-film state, which is a unique feature of the compressed film model. Earlier work by

Ruehl and coworkers successfully used a van der Waals equation of state to model the behavior of organic

and inorganic mixed droplets at high relative humidity (Ruehl and Wilson, 2014), demonstrating the effect

of surface tension following the onset of film formation once sufficient organic material was present. While

230   we know the factors that contribute to the equation of state and isotherm for well controlled systems the

enormous complexity of atmospheric aerosol presents a significant challenge in developing and utilizing a

predictive general model or theoretical framework.

The equilibrium gas–particle partitioning and liquid–liquid phase separation model is based on the Aerosol

Inorganic-Organic Mixtures Functional groups Activity Coefficients (AIOMFAC) model (Zuend et al.,

235   2008, 2011), coupled to a relatively simple, phase composition- and morphology-specific surface tension

model. This approach, used by Ovadnevaite and coworkers (Ovadnevaite et al., 2017), shows promise due

to its ability to predict the existence of a surface tension activation effect consistent with CCN observations

taken in marine air containing a nascent ultrafine aerosol size mode. In that study, enhanced CCN activity

of ultrafine particles was observed for aerosols consisting of organic material mixed with inorganic salts

240   and acids in North Atlantic marine air masses, which could not be explained when accounting for

hygroscopicity or solubility alone (when assuming surface tension of water). While the LLPS-based model

and the compressed film model of Ruehl et al. employ different principles and descriptions to account for

the surface composition, both agree that gradual surface tension changes dominate the CCN activation

process. Interestingly, while the observations of Ruehl et al. showed activation occurring when the surface

245   tension returns to its maximum value (i.e. that of pure water), the phase separation model predicted

activation prior to the surface tension returning to its maximum (for ultrafine particles). As discussed by

Ovadnevaite et al. (2017), this difference in the surface tension value reached at the point of CCN activation

depends in some cases on the size range of the (dry) particles considered (for the same dry composition).

Ovadnevaite et al. show that for particles of larger dry diameters (e.g. 175 nm for the case of their aerosol

250   model system), CCN activation is predicted to occur at a point where the particle's surface tension has

reached the value of pure water (see the Supplementary Information of that study). Hence, both observations

are consistent with the picture developed in Figure 1B and the details depend on the particle size range and

functional form describing the change in surface tension of the system considered. Moreover, it is important

to recognize that – regardless of whether the surface tension is equivalent to or lower than that of pure water

255   at the CCN activation point – a CCN exhibiting an evolving, lowered surface tension while approaching

the activation point during hygroscopic growth will activate at a lower supersaturation than a CCN of

constant surface tension equivalent to the pure-water value, since the former activates at a larger diameter,

as is evident from the examples of the red and green Kohler curves shown in Fig. 1B. This predicted size

effect indicates that it is not generally valid to assume that all activating CCN will have a surface tension

260   equivalent to or close to that of pure water – nor is it appropriate to use a single measurement of the surface

tension of a multicomponent CCN of known dry composition at its activation size (only) to determine its

Köhler curve. Furthermore, these model predictions also suggest that measurements of the surface tension

of larger CCN particles (e.g. > 150 nm dry diameter) may not allow for conclusions about the surface

tension of much smaller CCN, e.g. of 50 nm dry diameter.

265   **4 Identifying Surface Tension Effects from Critical Supersaturation**

Although the LLPS-based and compressed film model of CCN activation have had some success in

capturing surface tension effects, there remain substantial challenges in developing a generalized theory.

One challenge is that CCN techniques do not measure surface tension directly but instead observe the effects

of changes in surface tension, which may often be attributed to other factors. In order to identify surface

270   tension effects using these techniques, experiments must be performed to maximize the scope of surface

tension effects while minimizing changes in other variables that might influence observations. Here, we

propose new experiments, using a model system as an example, which allows surface tension effects to be

identified in the absence of other complicating factors.

Atmospheric
Chemistry
and Physics
Discussions

Using a Cloud Condensation Nucleus Counter (CCNC, Droplet Measurement Technology), we measured

275   the supersaturation required to activate mixed suberic acid and ammonium sulfate particles. Suberic acid

was chosen to represent low solubility oxygenated organic material typical of atmospheric secondary

organic aerosol. It is not a traditional surfactant, but its role in suppressing surface tension and modifying

the shape of the Kohler curve has been previously identified (Ruehl et al., 2016). Ammonium sulfate

particles were generated using an atomizer and dried using silica gel and a Nafion drier with dry N_2 counter

280   flow. The size distribution was measured and a size-selected seed was introduced into a flow tube

containing suberic acid and housed within a furnace oven. The temperature was set to volatilize the organic

material and allow it to condense onto the seed particles up to a desired thickness. The coated particles were

size-selected again and introduced into a particle counter and a Cloud Condensation Nucleus Counter

(CCNC; Droplet Measurement Technologies) at a concentration of around 2000 cm^{-3}. The activated fraction

285   was measured as a function of saturation ratio and the critical supersaturation was determined from the half-

rise times of a sigmoid fit to the data. A range of dry particle sizes and organic volume fractions (f_{org}) were

selected for measurements under humidified conditions at room temperature (~ 20 ℃). Notably, the coated

particle (i.e. total size) of the aerosol in its dry state was kept constant across a dataset spanning a range of

organic volume fractions. The CCNC was calibrated with ammonium sulfate particles at room temperature

290   at regular intervals, although typically the calibration remained stable during continued usage.

The organic volume fraction (f_{org}) was varied while maintaining fixed dry particle sizes, ensuring that any

surface tension effect would not be masked by changes in the overall size, in contrast to other studies that

allow both coated particle size and organic volume fraction to vary simultaneously (eg. (Hings et al., 2008;

Nguyen et al., 2017)). Figure 2A shows the critical supersaturation as a function of f_{org} for 100 nm (dry

295   diameter) mixed ammonium sulfate and suberic acid particles. Remarkably, despite the much lower

hygroscopicity of suberic acid relative to ammonium sulfate, there is very little increase in the required

supersaturation as the organic volume fraction increases (while the ammonium sulfate volume fraction is

reduced accordingly). In fact, considering a fixed surface tension of pure water, a κ_{org} value of 0.35 for the

organic fraction is required to explain these data (using $\kappa = 0.62$ for ammonium sulfate). This κ_{org} value is

300 lower than that reported by Ruehl et al. (where $\kappa_{org} = 0.5$), although those measurements were performed

on 150 nm particles at $f_{org} = 0.963$. If we apply the compressed film model (using the parameters established

in (Ruehl et al., 2016) for 150 nm particles at $f_{org} = 0.963$) to predict the critical supersaturation as a function

of f_{org}, we obtain a dependence that shows a peak SS_{crit} at $f_{org} = 0.4$ (Figure 2), followed by a decrease

towards higher f_{org}. This shape is consistent with the lower value of SS_{crit} reported by Ruehl et al. at $f_{org} =$

305 0.963. Although it does not reproduce the data exactly, it does more closely predict the observations across

the full range of composition. If we use the ideal molar volume derived κ_{org} value of 0.131 and a constant

surface tension of $\sigma = \sigma_w$, the bulk solubility prediction significantly overestimates SS_{crit} for $f_{org} > 0.5$. It

must be noted here that without prior knowledge that suberic acid is inherently of very low hygroscopicity

and exhibits low water-solubility, the prediction using $\kappa_{org} = 0.35$ could be mistaken as the correct answer.

310 However, a κ_{org} value of this magnitude is unphysical when considering the original definition of κ. One

could ignore the physical meaning of κ and simply use it as an all-encompassing parameter to describe

activation efficiency. In this case, the generality of the parameter to interpret observations in different

conditions is lost. For example, Figure 2B shows the same system of ammonium sulfate and suberic acid,

this time using 40 nm dry diameter particles. In this case, the required supersaturation decreases with

315 increasing organic fraction, suggesting that suberic acid is more hygroscopic than ammonium sulfate

(requiring $\kappa_{org} = 0.72$). For the ultrafine aerosol size reported here, the compressed film model does a worse

job at predicting the behavior, suggesting that it too suffers from a lack of generality in its applicability.

What is clear, however, is that a specific suberic acid hygroscopicity alone cannot explain the observations

across a range of particle sizes and compositions.

320 These observations are obscured when the data is reported with a fixed inorganic seed size with an

increasing organic fraction achieved through an increase in the coated diameter. The data as a function of

f_{org} with a fixed total diameter was used to plot SS_{crit} as a function of f_{org} with a fixed inorganic seed size,

shown in Figure 2C with an arbitrarily chosen inorganic seed size of 33 nm dry diameter. The value of SS_{crit}

for coated diameters 40, 50 and 100 nm was found by linear interpolation of the data in Figures 2A and 2B

325 (and the 50 nm case in Figure 3). The data is compared against a bulk κ-Köhler prediction, which exhibits

a similar trend, although with a slightly smaller slope when $\kappa_{org} = 0.15$. These data are brought to agreement

using $\kappa_{org} = 0.4$. However, we have already shown that for the 40 nm case, a value of κ_{org} greater than that

of AS is required to explain the data as a function of f_{org} with a fixed dry diameter. Specifically, in Fig. 2C,

the organic volume fractions are distinctly different for the three points shown: $f_{org} = 0.40$, 0.70, and 0.96

330 for the 40, 50, and 100 nm coated diameter cases, respectively. Thus, there is a clear loss of information

simply due to the choice of experimental procedure or data presentation.

For both sets of measurements, we also applied three model predictions based on the Aerosol Inorganic-

Organic Mixtures Functional groups Activity Coefficients (AIOMFAC) (Zuend et al., 2008, 2011) model

with LLPS and a phase-specific surface tension mixing rule considered. The full equilibrium calculation,

335 labeled as AIOMFAC-EQUIL in Figure 2, considers the potential existence of a bulk liquid–liquid

equilibrium, resulting in two liquid phases of distinct compositions yet each containing some amounts of

all three components. The chemical compositions affect the surface tensions of the individual phases and,

using a core-shell morphology assumption and minimum phase (film) thickness, that of the overall droplet.

For the calculations performed, suberic acid is assumed to be in a liquid state at high water activity. This

340 model predicts an LLPS for the aqueous suberic acid + ammonium sulfate system, but only up to a certain

water activity level < 0.99, beyond which a single liquid phase is the stable state. The upper limit of LLPS

predicted increases with the fraction of suberic acid in the system: LLPS onset $a_w \approx 0.942$ for $f_{org} = 0.27$ to

$a_w \approx 0.983$ for $f_{org} = 0.88$. This results in the absence of LLPS at supersaturated conditions prior to CCN

activation for both dry particle diameters considered. Therefore, the AIOMFAC-EQUIL prediction does

345 not lead to a significant surface tension reduction here, which explains why the predicted SS_{crit} in Fig. 2 is

similar to that of an iso-σ κ-Köhler model with $\kappa_{org} \approx 0.13$. The two AIOMFAC-CLLPS variants represent

simplified model calculations in which the assumption is made that dissolved aqueous electrolytes and

organics always reside in separate phases regardless of water content. In the variant labeled AIOMFAC-

CLLPS (w/ org film), all organic material is assumed to reside in a water-free organic shell-phase (an

350   organic film) at the surface of the aqueous droplet. This assumption leads to a maximum possible surface

tension lowering up to relatively large droplet sizes (for intermediate to high f_{org}), yet a reduced solute

effect, especially for high f_{org}. The variant labelled AIOMFAC-CLLPS (w/o org film) in Fig. 2 differs by

allowing water to partition to the organic-rich shell phase (in equilibrium with the target water activity),

which may affect the surface tension of that phase. Due to a significant water uptake by suberic acid,

355   predicted to occur for $a_w > 0.99$, the resulting surface tension prior to and near activation is that of pure

water and the SS_{crit} prediction resembles that of the AIOMFAC-EQUIL case. Physical parameters used in

these simulations are presented in Table 1 and a schematic representation of these cases is shown in Figure

A1. A comparison of predicted Köhler curves from these model variants is shown in Fig. A2 for the case

of $f_{org} = 0.58$. The AIOMFAC-based predictions of critical dry diameters and SScrit are listed in Table 2

360   for a range of dry diameters. A comparison of the different models with experimental data in Fig. 2 indicate

that for $f_{org} > 0.3$, the simplified organic film model variant AIOMFAC-CLLPS (w/ org film) offers the best

agreement with the measurements. This hints at a significant suppression of surface tension by suberic acid,

which is likely highly enriched at the droplet surface.

However, neither of the models fully captures the observed behavior at all f_{org} and size regimes. As discussed

365   by Ovadnevaite and coworkers (Ovadnevaite et al., 2017), the AIOMFAC-EQUIL and AIOMFAC-CLLPS

(w/ org film) calculations may provide upper and lower bounds on the prediction of SS_{crit} for a given system,

which is roughly in agreement with the data in Fig. 2. In reality, it is likely that some portion of suberic

acid dissolves into the aqueous droplet bulk at high relative humidity, itself contributing to the water uptake

of the droplet, as predicted by AIOMFAC-EQUIL, while a significant organic enrichment prevails at the

370   surface, lowering the surface tension and consequently SS_{crit}. Such behavior could explain the data and the

increasing model-measurement deviations towards higher f_{org}. Improvements of the AIOMFAC-based

models with more sophisticated bulk–surface partitioning treatments in individual liquid phases seem to

offer a way forward to address some of the observed shortcomings in future work. At this point, it remains

intriguing that the simplified organic film model provides the best description of these experimental data,

375   even though its restrictive assumptions about phase separation and organic water content seem to make it a

less physically realistic model variant.

These types of experiment also expose further factors that influence CCN activation, possibly through

modification to surface partitioning, such as the role of inorganic ions. We performed additional

measurements using different inorganic seed particles coated with suberic acid and observed vastly different

380   behavior across three different salts (ammonium sulfate, sodium iodide and sodium carbonate), shown in

Figure 3 for 50 nm dry diameter particles. We see for ammonium sulfate the same qualitative behavior as

for the other two sizes already discussed; in contrast, the responses of the systems containing the other salts

(all with suberic acid as the organic component) are very different. Sodium carbonate exhibits an increase

in the required critical supersaturation across the range of compositions; a trend that could reasonably be

385   predicted without invoking surface tension effects. The trend with sodium iodide is more complex and

appears to show a sharp discontinuity near $f_{org} = 0.5$, which was highly reproducible across multiple repeat

experiments over multiple days. These salts were chosen to span the range of the Hofmeister series, which

describes the propensity of inorganic ions to salt in or salt out organic molecules (proteins in particular).

Sulfate and carbonate are the best salting-out ions, while iodide has a relatively weak salting-out effect due

390   to its own surface propensity (Dos Santos et al., 2010). It is interesting to note the differences between

carbonate and sulfate, despite their similar position on the Hofmeister scale. The role of the cation is

generally considered to be much smaller than that of the anion, thus these differences are non-trivial. These

results serve to further highlight a key conclusion of this work – that we currently lack a robust molecular

model that is capable of describing and therefore accurately predicting CCN hygroscopicity and activation

395   even in a relatively simple model system. We hope to prompt further discussions and experimental studies

to explore these observations and bulk/surface composition effects on surface tension and CCN activation

in more detail.

5 Summary and Conclusions

Surface tension effects can lead to significant differences from classic, hygroscopicity mixing rule

400   mechanisms for CCN activation. While it has already been made clear that the activation diameter can be

significantly different from that determined by an *iso-σ* Köhler curve, in this work we reveal the potential

for more subtle changes in CCN activity (both increases and decreases relative to pure ammonium sulfate

particles) as a result of the organics-influenced surface tension evolution during droplet growth. These

changes were captured by measuring particles at a fixed diameter with a range of organic volume fractions.

405   Ultimately, to derive an accurate picture of CCN activity across the relevant ranges of chemical

compositions and size distributions, the effects of surface tension variability must be taken into account. It

should be noted, however, that there are many situations where using simple mixing rules with inferred

values for κ_{org} can lead to sufficiently accurate predictions without the need for more complex analyses or

simulations. It is therefore of key importance to constrain the conditions under which simple approaches

410   are justified – and to know when they may be inappropriate. Taking the activation model based on Köhler

theory forward will require a more rigorous interrogation of the role of co-solutes in partitioning, and

ultimately an assessment of its effect in real-world simulations of cloud formation.

In the meantime, it is important for environmental scientists to recognize the conditions in which surface

effects may be influencing cloud droplet formation, e.g., low solubility or insoluble organics mixed with

415   inorganic salts, high-RH phase separation, small particle sizes with critical supersaturations close to the

peak supersaturations experienced in clouds, etc. We suggest, if possible, that experimental data be explored

as a function of organic volume fraction while keeping the overall dry particle size the same, as from our

laboratory experiments this dependence shows the most clear indicator of an unexplained size effect that

may be attributed to bulk–surface partitioning. In experiments where both size and composition vary, the

420   contribution from each is less clear and the effect of the organic component due to bulk–surface partitioning

could be hidden. Further fundamental laboratory and modeling studies being performed will allow for in-

depth testing and refinements of the proposed models and mechanisms that describe bulk–surface

partitioning and surface tension, ultimately reaching towards a robust and universal mechanism that allows both hygroscopicity and surface tension effects to be coupled into a practical framework.

Atmospheric
Chemistry
and Physics
Discussions

Open Access

EGU

References

Abdul-Razzak, H. and Ghan, S. J.: A parameterization of aerosol activation: 2. Multiple aerosol types, J. Geophys. Res., 105, 6837–6844, 2000.

435 Asa-Awuku, A. and Nenes, A.: Effect of solute dissolution kinetics on cloud droplet formation: Extended Köhler theory, J. Geophys. Res., 112(D22201), D22201, doi:10.1029/2005JD006934, 2007.

Asa-Awuku, A., Sullivan, A. P., Hennigan, C. J., Weber, R. J. and Nenes, A.: Investigation of molar volume and surfactant characteristics of water-soluble organic compounds in biomass burning aerosol, Atmos. Chem. Phys., 8(4), 799–812, doi:10.5194/acp-8-799-2008, 2008.

440 Asa-Awuku, A., Engelhart, G. J., Lee, B. H., Pandis, S. N. and Nenes, A.: Relating CCN activity, volatility, and droplet growth kinetics of β-caryophyllene secondary organic aerosol, Atmos. Chem. Phys., 9(3), 795–812, doi:10.5194/acp-9-795-2009, 2009.

Boyer, H. C. and Dutcher, C. S.: Atmospheric Aqueous Aerosol Surface Tensions: Isotherm-based Modeling and Biphasic Microfluidic Measurements, , doi:10.1021/ACS.JPCA.7B03189, 2017.

445 Boyer, H. C., Bzdek, B. R., Reid, J. P. and Dutcher, C. S.: A Statistical Thermodynamic Model for Surface Tension of Organic and Inorganic Aqueous Mixtures, J. Phys. Chem. A, acs.jpca.6b10057, doi:10.1021/acs.jpca.6b10057, 2016.

Clegg, S. L. and Wexler, A. S.: Densities and apparent molar volumes of atmospherically important electrolyte solutions. I. The solutes H2SO4, HNO3, HCl, Na2SO4, NaNO3, NaCl, (NH4)2SO4, 450 NH4NO3, and NH4Cl from 0 to 50 °C, including extrapolations to very low temperature and to the pure l, J. Phys. Chem. A, 115(15), 3393–3460, 2011.

Collins, D. B., Bertram, T. H., Sultana, C. M., Lee, C., Axson, J. L. and Prather, K. A.: Phytoplankton blooms weakly influence the cloud forming ability of sea spray aerosol, Geophys. Res. Lett., 43(18), 9975–9983, doi:10.1002/2016GL069922, 2016.

455 Facchini, M., Mircea, M., Fuzzi, S. and Charlson, R.: Cloud albedo enhancement by surface-active organic solutes in growing droplets, Nature, 401, 257–259 [online] Available from: http://www.nature.com/nature/journal/v401/n6750/abs/401257a0.html (Accessed 3 December 2013), 1999.

Forestieri, S. D., Staudt, S. M., Kuborn, T. M., Faber, K., Ruehl, C. R., Bertram, T. H. and Cappa, C. D.: 460 Establishing the Impact of Model Surfactants on Cloud Condensation Nuclei Activity of Sea Spray

Atmospheric
Chemistry
and Physics
Discussions

Aerosols, Atmos. Chem. Phys. Discuss, 207, 1–44, 2018.

Fuentes, E., Coe, H., Green, D. and McFiggans, G.: On the impacts of phytoplankton-derived organic matter on the properties of the primary marine aerosol - Part 2: Composition, hygroscopicity and cloud condensation activity, Atmos. Chem. Phys., 11(6), 2585–2602, doi:10.5194/acp-11-2585-2011, 2011.

465   Good, N., Topping, D. O., Allan, J. D., Flynn, M., Fuentes, E., Irwin, M., Williams, P. I., Coe, H. and McFiggans, G.: Consistency between parameterisations of aerosol hygroscopicity and CCN activity during the RHaMBLe discovery cruise, Atmos. Chem. Phys., 10(7), 3189–3203, doi:10.5194/acp-10-3189-2010, 2010.

Hings, S. S., Wrobel, W. C., Cross, E. S., Worsnop, D. R., Davidovits, P. and Onasch, T. B.: CCN
470   activation experiments with adipic acid: Effect of particle phase and adipic acid coatings on soluble and insoluble particles, Atmos. Chem. Phys., 8(14), 3735–3748, doi:10.5194/acp-8-3735-2008, 2008.

Jura, G. and Harkins, W. D.: Surfaces of solids. XIV. A Unitary Thermodynamic Theory of the Adsorption of Vapors on Solids and of Insoluble Films on Liquid Subphases, J. Am. Chem. Soc., 68(10), 1941–1952, doi:10.1021/ja01214a022, 1946.

475   Köhler, H.: The nucleus in and the growth of hygroscopic droplets, Trans. Faraday Soc., 32(0), 1152–1161, doi:10.1039/TF9363201152, 1936.

Kuwata, M., Shao, W., Lebouteiller, R. and Martin, S. T.: Classifying organic materials by oxygen-to-carbon elemental ratio to predict the activation regime of Cloud Condensation Nuclei (CCN), Atmos. Chem. Phys., 13(10), 5309–5324, doi:10.5194/acp-13-5309-2013, 2013.

480   Li, Z., Williams, A. and Rood, M.: Influence of soluble surfactant properties on the activation of aerosol particles containing inorganic solute, J. Atmos. Sci., 55, 1859–1866 [online] Available from: http://journals.ametsoc.org/doi/abs/10.1175/1520-0469(1998)055%3C1859:IOSSPO%3E2.0.CO;2 (Accessed 28 November 2013), 1998.

McFiggans, G., Artaxo, P., Baltensperger, U., Coe, H., Facchini, M. C., Feingold, G., Fuzzi, S., Gysel,
485   M., Laaksonen, A., Lohmann, U., Mentel, T. F., Murphy, D. M., O'Dowd, C. D., Snider, J. R. and Weingartner, E.: The effect of physical and chemical aerosol properties on warm cloud droplet activation, Atmos. Chem. Phys., 6, 2593–2649, 2006.

Nguyen, Q. T., Kjær, K. H., Kling, K. I., Boesen, T. and Bilde, M.: Impact of fatty acid coating on the CCN activity of sea salt particles, Tellus, Ser. B Chem. Phys. Meteorol., 69(1), 1–15,
490   doi:10.1080/16000889.2017.1304064, 2017.

Nozière, B., Baduel, C. and Jaffrezo, J.-L.: The dynamic surface tension of atmospheric aerosol surfactants reveals new aspects of cloud activation, Nat. Comm., 5(3335), 1–7, doi:10.1038/ncomms4335, 2014.

Ovadnevaite, J., Ceburnis, D., Martucci, G., Bialek, J., Monahan, C., Rinaldi, M., Facchini, M. C.,
495   Berresheim, H., Worsnop, D. R. and O'Dowd, C.: Primary marine organic aerosol: A dichotomy of low hygroscopicity and high CCN activity, Geophys. Res. Lett., 38(21), 1–5, doi:10.1029/2011GL048869, 2011.

Ovadnevaite, J., Zuend, A., Laaksonen, A., Sanchez, K. J., Roberts, G., Ceburnis, D., Decesari, S., Rinaldi, M., Hodas, N., Facchini, M. C., Seinfeld, J. H. and O? Dowd, C.: Surface tension prevails over
500   solute effect in organic-influenced cloud droplet activation, Nature, 546(7660), 637–641, doi:10.1038/nature22806, 2017.

Petters, M. D. and Kreidenweis, S. M.: A single parameter representation of hygroscopic growth and cloud condensation nucleus activity, Atmos. Chem. Phys., 13(2), 1081–1091, doi:10.5194/acpd-8-5939-2008, 2007.

505   Petters, M. D. and Kreidenweis, S. M.: A single parameter representation of hygroscopic growth and cloud condensation nucleus activity – Part 3: Including surfactant partitioning, Atmos. Chem. Phys., 13, 1081–1091, doi:10.5194/acpd-8-5939-2008, 2013.

Petters, M. D., Kreidenweis, S. M. and Ziemann, P. J.: Prediction of cloud condensation nuclei activity for organic compounds using functional group contribution methods, Geosci. Model Dev., 9(1), 111–124,
510   doi:10.5194/gmd-9-111-2016, 2016.

Petters, S. S. and Petters, M. D.: Surfactant effect on cloud condensation nuclei for two-component internally mixed aerosols, J. Geophys. Res. Atmos., 121, 1878–1895, doi:10.1002/2015JD024090.Received, 2016.

Prisle, N. L., Raatikainen, T., Sorjamaa, R., Svenningsson, B., Laaksonen, A. and Bilde, M.: Surfactant
515   partitioning in cloud droplet activation: A study of C8, C10, C12 and C14 normal fatty acid sodium salts, Tellus, Ser. B Chem. Phys. Meteorol., 60 B(3), 416–431, doi:10.1111/j.1600-0889.2008.00352.x, 2008.

Prisle, N. L., Raatikainen, T., Laaksonen, A. and Bilde, M.: Surfactants in cloud droplet activation: Mixed organic-inorganic particles, Atmos. Chem. Phys., 10(12), 5663–5683, doi:10.5194/acp-10-5663-2010, 2010.

520   Rastak, N., Pajunoja, A., Acosta Navarro, J. C., Ma, J., Song, M., Partridge, D. G., Kirkevåg, A., Leong,

Y., Hu, W. W., Taylor, N. F., Lambe, A., Cerully, K., Bougiatioti, A., Liu, P., Krejci, R., Petäjä, T., Percival, C., Davidovits, P., Worsnop, D. R., Ekman, A. M. L., Nenes, A., Martin, S., Jimenez, J. L., Collins, D. R., Topping, D. O., Bertram, A. K., Zuend, A., Virtanen, A. and Riipinen, I.: Microphysical explanation of the RH-dependent water affinity of biogenic organic aerosol and its importance for

525 climate, Geophys. Res. Lett., 44(10), 5167–5177, doi:10.1002/2017GL073056, 2017.

Renbaum-Wolff, L., Song, M., Marcolli, C., Zhang, Y., Liu, P. F., Grayson, J. W., Geiger, F. M., Martin, S. T. and Bertram, a. K.: Observations and implications of liquid–liquid phase separation at high relative humidities in secondary organic material produced by α-pinene ozonolysis without inorganic salts, Atmos. Chem. Phys., 16, 7969–7979, doi:10.5194/acpd-15-33379-2015, 2016.

530 Riipinen, I., Koponen, I. K., Frank, G. P., Hyvärinen, A.-P., Vanhanen, J., Lihavainen, H., Lehtinen, K. E. J., Bilde, M. and Kulmala, M.: Adipic and Malonic Acid Aqueous Solutions: Surface Tensions and Saturation Vapor Pressures, J. Phys. Chem. A, 111(50), 12995–13002, doi:10.1021/jp073731v, 2007.

Roberts, G. C. and Nenes, a.: A Continuous-Flow Streamwise Thermal-Gradient CCN Chamber for Atmospheric Measurements, Aerosol Sci. Technol., 39(3), 206–221, doi:10.1080/027868290913988,

535 2005.

Ruehl, C. R. and Wilson, K. R.: Surface organic monolayers control the hygroscopic growth of submicrometer particles at high relative humidity., J. Phys. Chem. A, 118(22), 3952–3966, doi:10.1021/jp502844g, 2014.

Ruehl, C. R., Davies, J. F. and Wilson, K. R.: An interfacial mechanism for cloud droplet formation on

540 organic aerosols, Science (80-.)., 351(6280), 1447–1450, 2016.

Dos Santos, A. P., Diehl, A. and Levin, Y.: Surface tensions, surface potentials, and the hofmeister series of electrolyte solutions, Langmuir, 26(13), 10778–10783, doi:10.1021/la100604k, 2010.

Sorjamaa, R., Raatikainen, T. and Laaksonen, A.: The role of surfactants in Köhler theory reconsidered, Atmos. Chem. Phys., 4, 2107–2117, doi:10.5194/acpd-4-2781-2004, 2004.

545 Topping, D., Connolly, P. and McFiggans, G.: Cloud droplet number enhanced by co-condensation of organic vapours, Nat. Geosci., 6, 443–446, doi:10.1038/ngeo1809, 2013.

Topping, D. O. and McFiggans, G.: Tight coupling of particle size, number and composition in atmospheric cloud droplet activation, Atmos. Chem. Phys., 12, 3253–3260, doi:10.5194/acp-12-3253-2012, 2012.

550 Topping, D. O., McFiggans, G. B., Kiss, G., Varga, Z., Facchini, M. C., Decesari, S. and Mircea, M.:

Surface tensions of multi-component mixed inorganic/organic aqueous systems of atmospheric significance: Measurements, model predictions and importance for cloud activation predictions, Atmos. Chem. Phys., 7(9), 2371–2398, doi:10.5194/acp-7-2371-2007, 2007.

Vargaftik, N. B., Volkov, B. N. and Voljak, L. D.: International Tables of the Surface Tension of Water, J. Phys. Chem. Ref. Data, 12(3), 817–820, doi:10.1063/1.555688, 1983.

Wang, C., Lei, Y. D., Endo, S. and Wania, F.: Measuring and Modeling the Salting-out Effect in Ammonium Sulfate Solutions, Environ. Sci. Technol., 48(22), 13238–13245, doi:10.1021/es5035602, 2014.

Yakobi-Hancock, J. D., Ladino, L. A., Bertram, A. K., Huffman, J. A., Jones, K., Leaitch, W. R., Mason, R. H., Schiller, C. L., Toom-Sauntry, D., Wong, J. P. S. and Abbatt, J. P. D.: CCN activity of size-selected aerosol at a Pacific coastal location, Atmos. Chem. Phys., 14(22), 12307–12317, doi:10.5194/acp-14-12307-2014, 2014.

Zuend, A., Marcolli, C., Luo, B. P. and Peter, T.: A thermodynamic model of mixed organic-inorganic aerosols to predict activity coefficients, Atmos. Chem. Phys., 8, 6069–6151, doi:10.5194/acpd-8-6069-2008, 2008.

Zuend, A., Marcolli, C., Booth, A. M., Lienhard, D. M., Soonsin, V., Krieger, U. K., Topping, D. O., McFiggans, G., Peter, T. and Seinfeld, J. H.: New and extended parameterization of the thermodynamic model AIOMFAC: calculation of activity coefficients for organic-inorganic mixtures containing carboxyl, hydroxyl, carbonyl, ether, ester, alkenyl, alkyl, and aromatic functional groups, Atmos. Chem. Phys., 11, 9155–9206, doi:10.5194/acp-11-9155-2011, 2011.

575 **Table 1: Value of physical parameters used in AIOMFAC calculations. Density of mixtures were calculated as a linear (additive) combination of the apparent molar volumes of the contributions of water, ammonium sulfate (AS), and suberic acid.**

Calculation parameter	Value	Unit
Temperature, T	293.15	K
Pure comp. surface tension water (at T) (Vargaftik et al., 1983)	72.75	mJ m^{-2}
Pure comp. surface tension Suberic Acid (at T) *	35.00	mJ m^{-2}
Pure comp. surface tension AS (at T) **	72.75	mJ m^{-2}
Density of pure water (liq.) at T	997	kg m^{-3}
Density of pure suberic acid (liq.) at T	1220	kg m^{-3}
Density of pure AS (liq.) at T (Clegg and Wexler, 2011)	1550	kg m^{-3}
Density of pure AS (solid) at T (Clegg and Wexler, 2011)	1770	kg m^{-3}
Minimum shell phase thickness, $\delta_{\beta,min}$	0.3	nm

*Value taken from measurements for of adipic acid (Riipinen et al., 2007) on the basis of structural similarity to suberic acid. **Assumption of no influence on droplet surface tension compared to water here

580 (since highly dilute).

Table 2: Critical supersaturation SS_{crit} (%) for given dry diameters ($D_{dry,crit}$) and organic volume fractions (f_{org}) in dry particle at T = 293.15 K; predicted by the different AIOMFAC-based models.

AIOMFAC-EQUIL; with liquid–liquid phase separation considered when predicted

Mixture		Dry diameter [nm] (of overall particle)											
Solutes	f_{org}	30	35	40	45	50	60	80	100	120	140	160	200
AS	0.00	1.005	0.788	0.639	0.532	0.451	0.339	0.217	0.154	0.116	0.091	0.074	0.053
Suberic + AS	0.27	1.135	0.893	0.726	0.605	0.513	0.387	0.248	0.176	0.133	0.105	0.085	0.061
Suberic + AS	0.40	1.214	0.957	0.779	0.649	0.552	0.416	0.267	0.190	0.143	0.113	0.092	0.066
Suberic + AS	0.58	1.350	1.068	0.871	0.727	0.619	0.468	0.301	0.214	0.162	0.128	0.105	0.074
Suberic + AS	0.75	1.532	1.214	0.993	0.831	0.708	0.537	0.347	0.247	0.187	0.148	0.121	0.086
Suberic + AS	0.88	1.751	1.389	1.136	0.951	0.811	0.616	0.399	0.285	0.216	0.172	0.140	0.100

585

AIOMFAC-CLLPS (w/ org film); organic phase assumed water-free

Suberic + AS	0.27	0.972	0.766	0.624	0.520	0.442	0.334	0.215	0.153	0.116	0.091	0.075	0.053
Suberic + AS	0.40	0.961	0.759	0.618	0.516	0.439	0.333	0.214	0.153	0.116	0.092	0.075	0.053
Suberic + AS	0.58	0.950	0.751	0.613	0.513	0.437	0.331	0.214	0.153	0.116	0.092	0.075	0.054
Suberic + AS	0.75	0.944	0.747	0.611	0.511	0.436	0.331	0.214	0.153	0.116	0.092	0.076	0.054
Suberic + AS	0.88	0.987	0.781	0.637	0.532	0.453	0.342	0.220	0.156	0.118	0.093	0.076	0.054

AIOMFAC-CLLPS (w/o org film); water uptake by organic-rich phase considered

Suberic + AS	0.27	1.108	0.878	0.716	0.598	0.509	0.385	0.247	0.176	0.133	0.105	0.085	0.061
Suberic + AS	0.40	1.197	0.948	0.774	0.646	0.550	0.416	0.267	0.190	0.144	0.113	0.092	0.066
Suberic + AS	0.58	1.357	1.075	0.877	0.733	0.624	0.472	0.303	0.216	0.163	0.129	0.105	0.075
Suberic + AS	0.75	1.579	1.246	1.017	0.849	0.723	0.547	0.352	0.250	0.189	0.150	0.122	0.087
Suberic + AS	0.88	1.999	1.592	1.303	1.089	0.926	0.697	0.443	0.301	0.220	0.174	0.142	0.101

590

Atmospheric
Chemistry
and Physics
Discussions

Open Access

Table 3: Experimentally measured critical supersaturation for given dry diameter, inorganic particle core, and organic volume fraction.

D_{dry} / nm	Inorganic	f_{org}	SS_{crit} (%)
100	$(NH_4)_2SO_4$	0.00	0.16
		0.27	0.17
		0.58	0.17
		0.88	0.19
40	$(NH_4)_2SO_4$	0.00	0.66
		0.33	0.62
		0.58	0.57
		0.88	0.60
50	$(NH_4)_2SO_4$	0.00	0.45
		0.27	0.45
		0.41	0.42
		0.66	0.41
		0.88	0.39
50	NaI	0.00	0.38
		0.27	0.41
		0.41	0.43
		0.49	0.45
		0.53	0.41
		0.56	0.41
		0.66	0.42
		0.78	0.45
		0.88	0.48
50	Na_2CO_3	0.00	0.33
		0.27	0.34
		0.49	0.35
		0.66	0.41
		0.78	0.42
		0.88	0.44

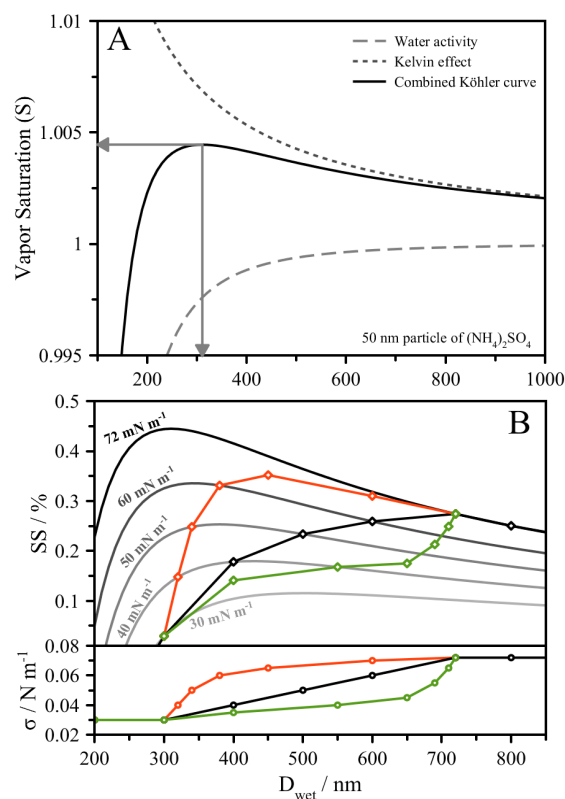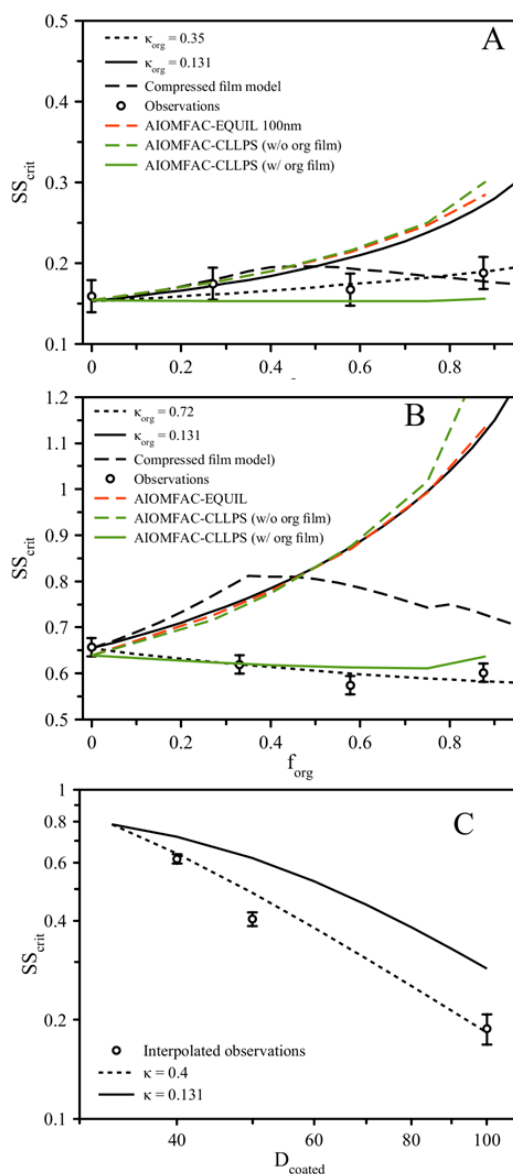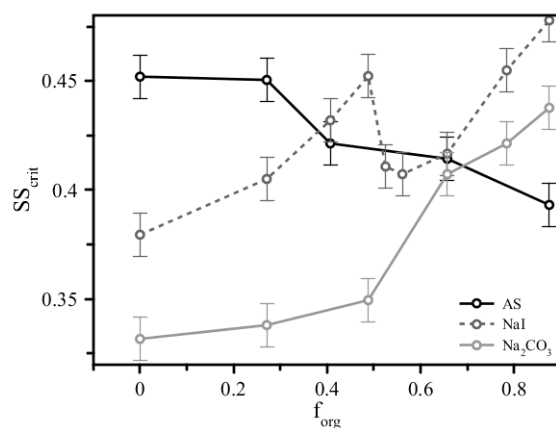Atmospheric
Chemistry
and Physics
Discussions

Figure 1: (A) Köhler curve construction from the combination of the water activity term and the Kelvin effect, shown here for 50 nm particles of ammonium sulfate. The arrows indicate the critical supersaturation (SS_{crit}) and the critical wet activation diameter (D_{crit}). (B) Köhler curves (NB. $SS = (S-1) \times 100$ %) of varying fixed surface tension values for 50 nm (dry diameter) particles with water activity treated as an ammonium sulfate solution. A schematic linear dependence of surface tension on droplet diameter is shown in black, and the Köhler curve construction that takes into account the change in surface tension is shown in bold and with diamond symbols. Additional surface tension dependencies are shown in red, which exhibits activation at $\sigma < \sigma_w$, and in green, which shows a dramatic increase in the critical wet diameter.

Atmospheric
Chemistry
and Physics
Discussions

Figure 2: (A) Measured critical supersaturation (SS_{crit}) of size-selected ammonium sulfate particles coated with suberic acid (points) to a set dry diameter of 100 nm at $T \approx 293$ K. The curves show predictions from the compressed film model of Ruehl et al., a simple κ-Köhler model with constant surface tension, and model variants from the AIOMFAC-based framework (see text). (B) Analogous to (A) but for particles of ammonium sulfate coated to 40 nm dry diameter by suberic acid. (C) Using the data from panels A and B, SS_{crit} is shown as a function of coated diameter with a fixed inorganic seed of 33 nm (points). The lines indicate the κ-Köhler model with constant surface tension using different but constant values of κ_{org}.

605

610

Figure 3: The measured critical supersaturation for 50 nm dry diameter particles comprised of different salts (ammonium sulfate, sodium iodide and sodium carbonate) and variable volume fractions of suberic acid (f_{org}) at $T \approx 293$ K.
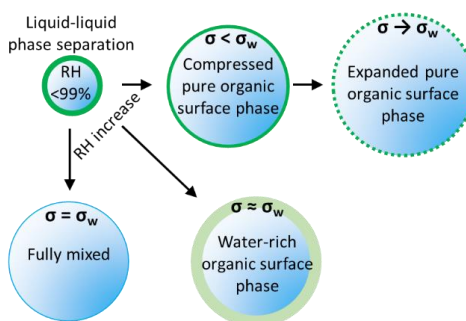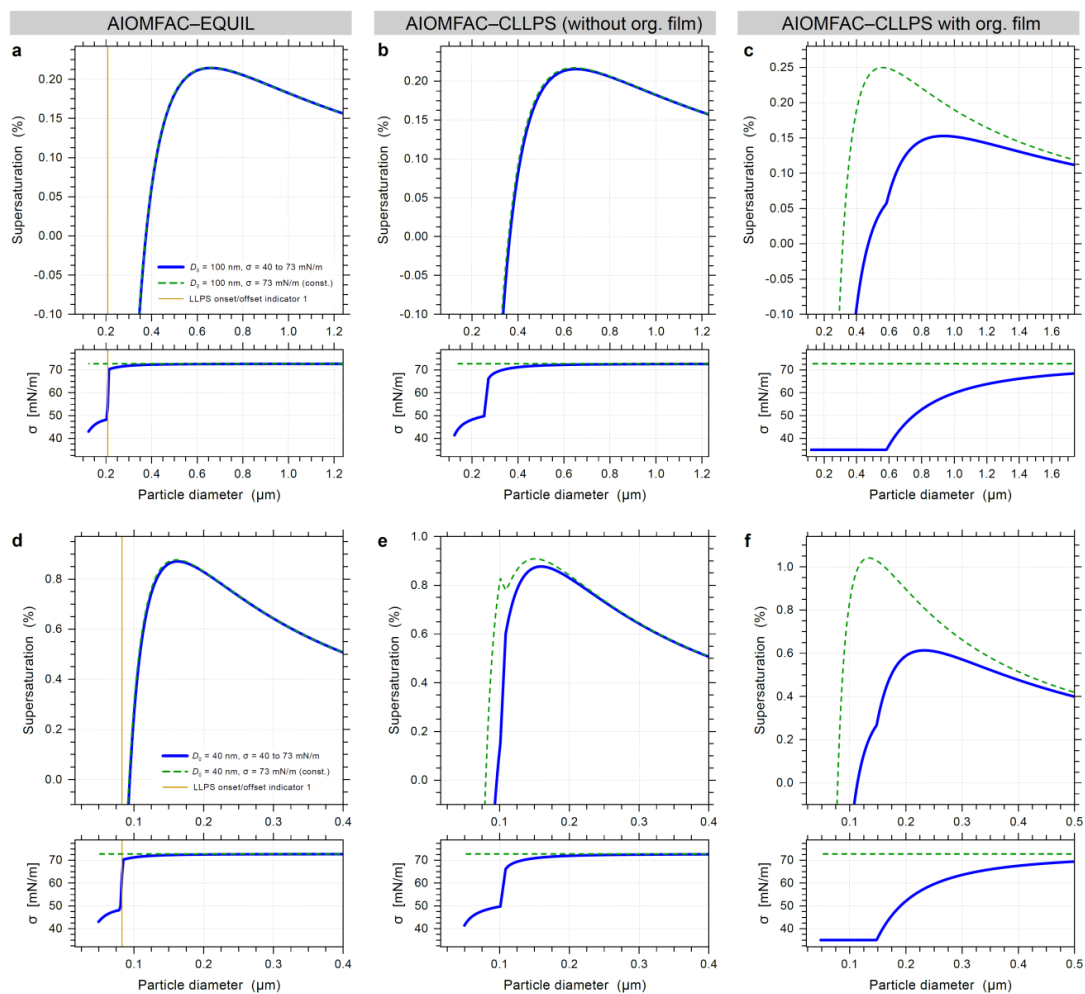
615   **Appendix**

Figure A1: Schematic representation of the three model variants. AIOMFAC-EQUIL treats the droplets as a fully mixed single phase, with the surface tension of the wet droplet sharply approaching

620   **σ_w. The phase separated variants considered a surface phase that is water-rich, with surface tension close to σ_w, and a surface phase that excludes water, behaving as an organic surface film, with $\sigma < \sigma_w$. The output from these scenarios are shown in Figure A2.**

625   **Figure A2: Predicted Köhler curves and associated droplet surface tensions for 100 nm (a, b, c) and 40 nm (d, e, f) dry**

diameter particles of ammonium sulfate with suberic acid at $f_{org} = 0.58$ using the AIOMFAC models described in the main

text. The AIOMFAC-CLLPS with org. film gives the closest predictions to the experimental observations and predicts

similar shaped curves to those measured experimentally by (Ruehl et al., 2016).